

Supporting Information

A perylenediimide-based nanocarrier monitors curcumin release with “off-on” fluorescence switch

Wenyu Cheng,^{a,b} Hongtao Chen,^a Chendong Ji,^a Ru Yang^{*b} and Meizhen Yin^{*a}

^a Beijing Laboratory of Biomedical Materials, Key Laboratory of Biomedical Materials of Natural Macromolecules, Ministry of Education, Beijing Advanced Innovation Center for Soft Matter Science and Engineering, BAIC-SM, Beijing University of Chemical Technology, 100029 Beijing, China.

E-mail: yinmz@mail.buct.edu.cn

^b State Key Laboratory of Chemical Resource Engineering, Beijing Key Laboratory of Electrochemical Process and Technology for Materials, Beijing University of Chemical Technology, Beijing 100029, China.

E-mail: ruyang@mail.buct.edu.cn

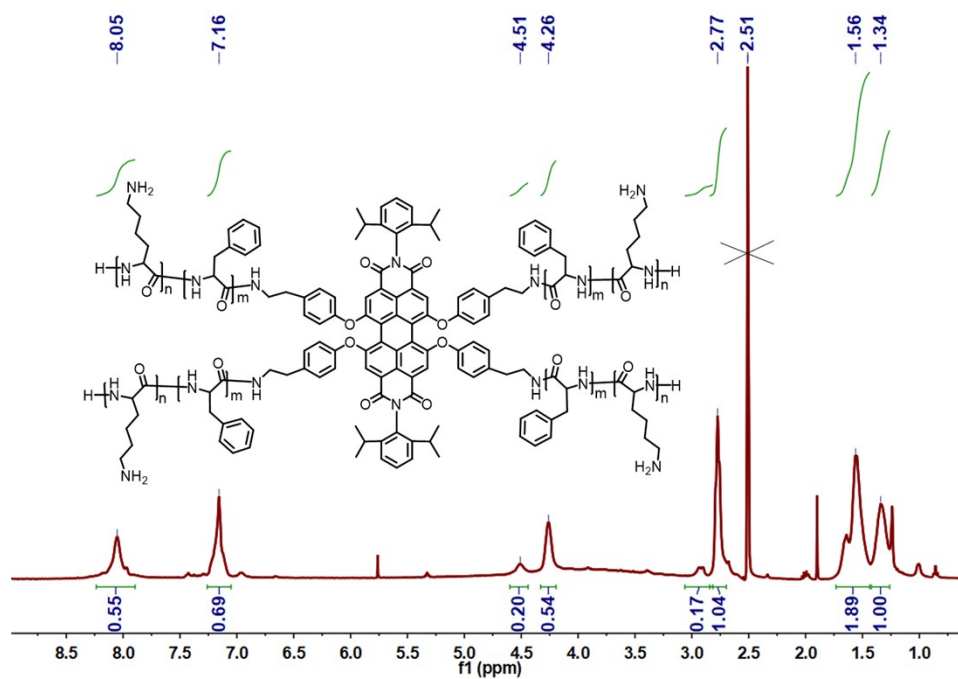
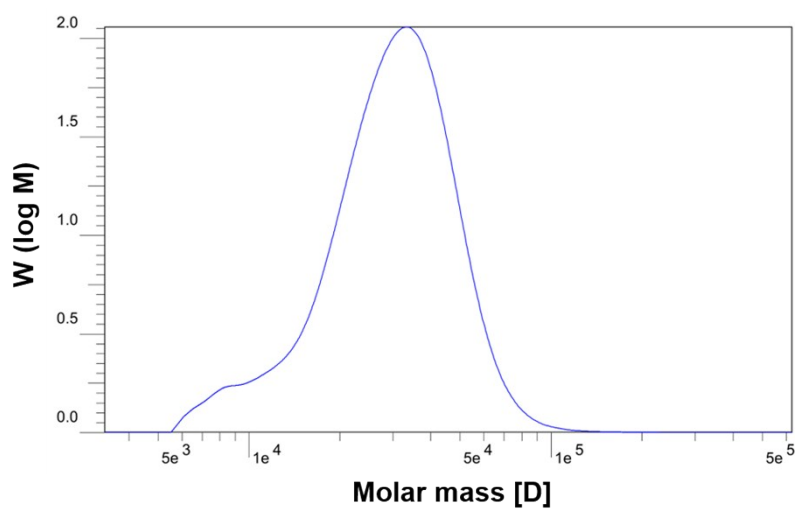


Fig. S1 ¹H NMR spectrum of PPL in DMSO-*d*₆.



| Mn | Mw | Mw/Mn |
|--------|--------|-------|
| 25,000 | 32,300 | 1.29 |

Fig. S2 Gel permeation chromatography of PPL.

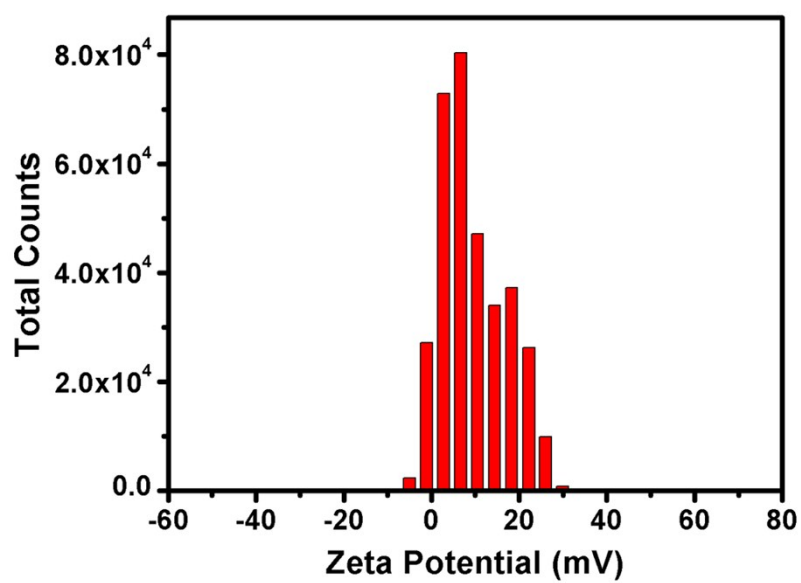


Fig. S3 Zeta potential of PPL-B.

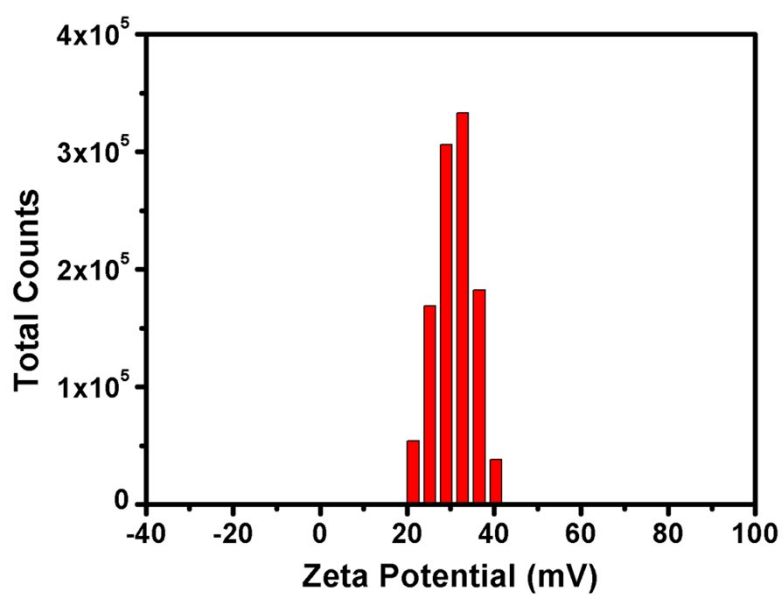


Fig. S4 Zeta potential of PPL.

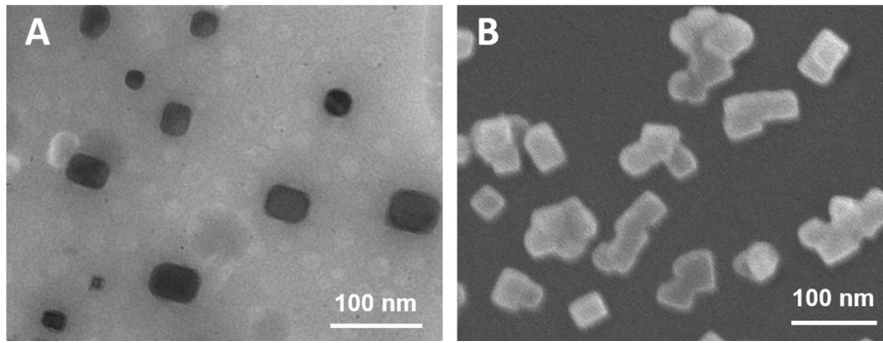


Fig. S5 TEM (A) and SEM (B) images of PPL-B self-assembly.

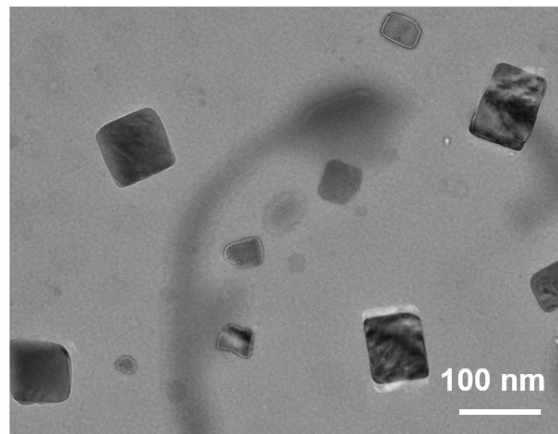


Fig. S6 TEM image of CUR@PPL-B self-assembly.

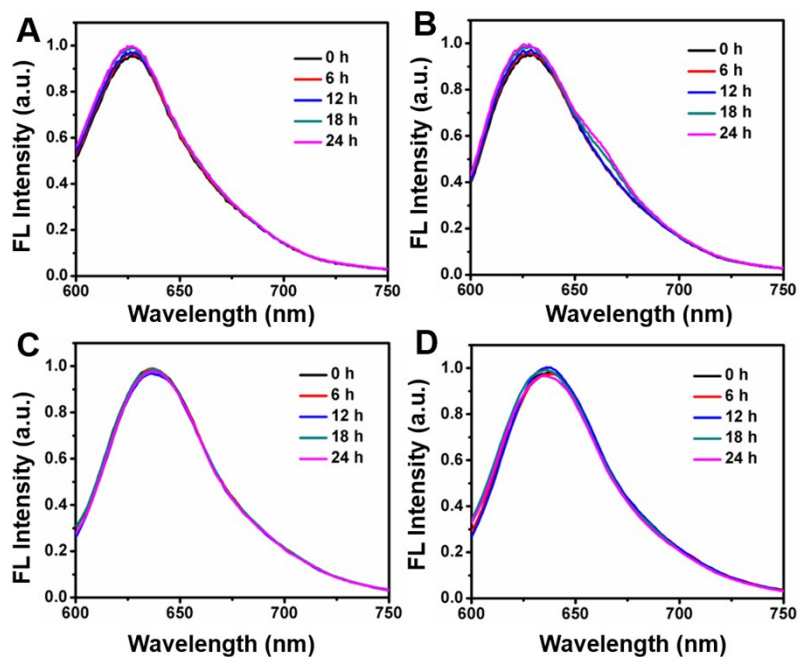


Fig. S7 Fluorescence intensity of CUR@PPL-B (10 μg/mL) in FBS and PBS at different storage time. (A) FBS, pH 5.0; (B) FBS, pH 7.4; (C) PBS, pH 5.0; (D) PBS, pH 7.4. With the increase of storage time, fluorescence of PPL-B remains unchanged, indicating good stability of CUR@PPL-B.

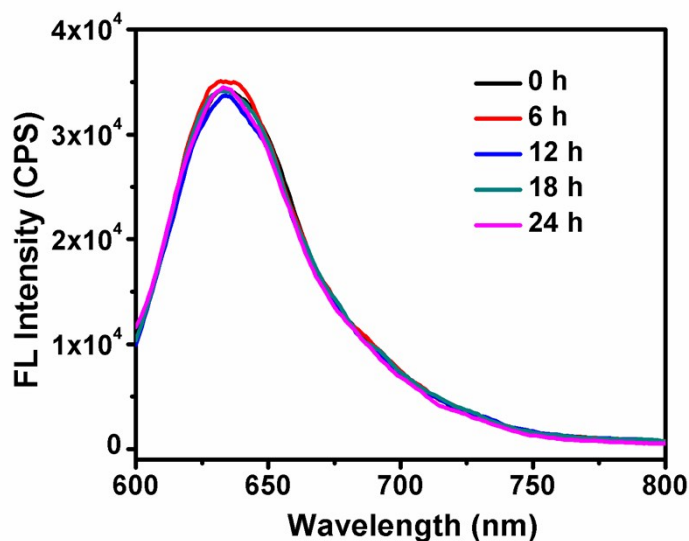


Fig. S8 Fluorescence intensity of CUR@PPL-B (1 μM) in PBS (PH = 7.4) at different storage time. Fluorescence of CUR@PPL-B maintains at quenched state for at least 24 h, indicating good stability of CUR@PPL-B in diluted solution.

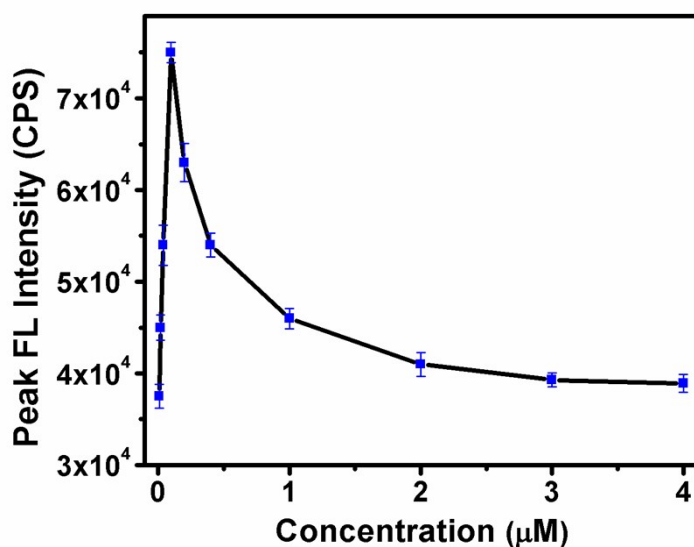


Fig. S9 Relationship between fluorescence intensity and concentration of CUR@PPL-B. The critical micelle concentration was detected to be 0.1 μM .

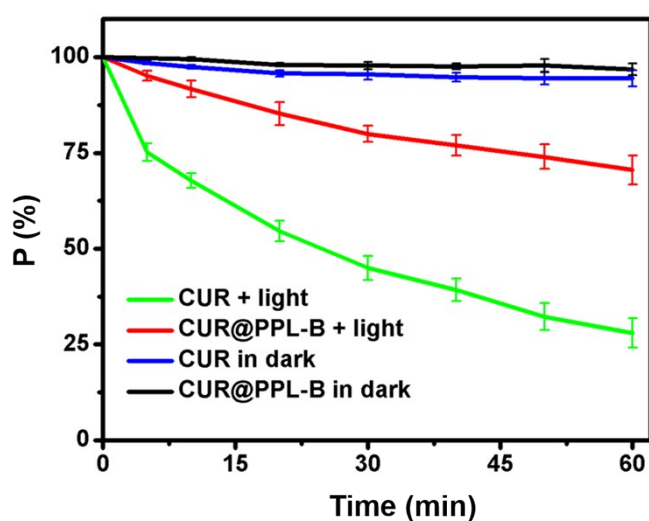


Fig. S10 Photostability of CUR and CUR@PPL-B. Vertical axis represents percentage ratio of remained absorption peak value.

Photostability of CUR@PPL-B

To ascertain whether nanocarrier CUR@PPL-B can stabilize curcumin (CUR) under light, photostability of pristine CUR and CUR@PPL-B were measured. Here we use the percentage of remained UV-Vis absorption peak value (P) of CUR to show its photostability. Thus, a smaller P indicates that CUR decompose more severely. Fig. S14 (ESI[†]) shows the relationship

between P and time. Obviously, CUR in nanocarrier decomposes slower than pristine CUR, proving that PPL-B can stabilize CUR under light irradiation.

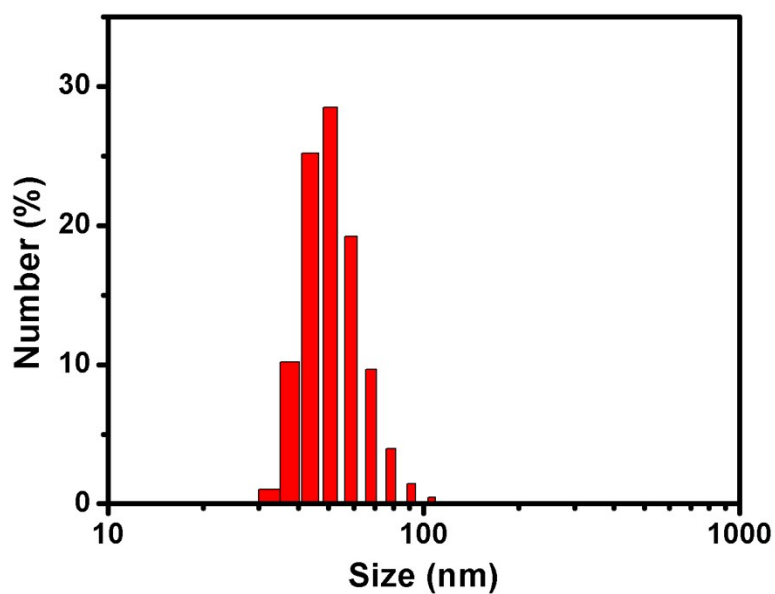


Fig. S11 Particle size of PPL-B measured by DLS.

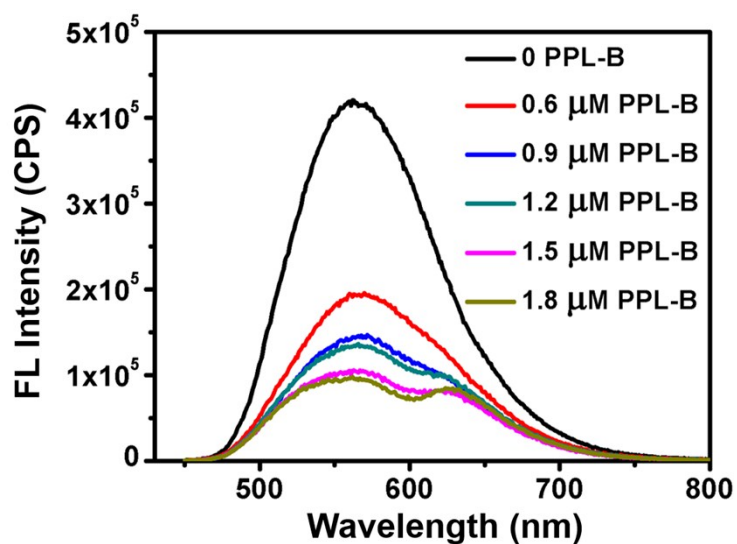


Fig. S12 Fluorescence quenching of curcumin by PPL-B.

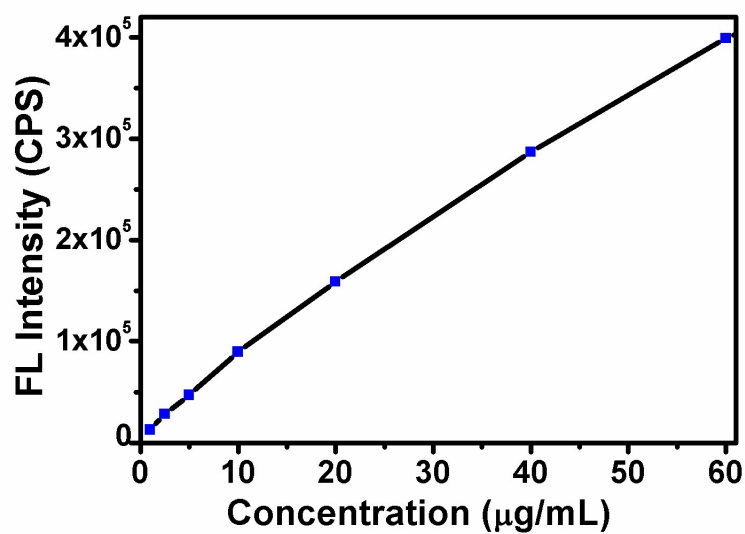


Fig. S13 Relationship between fluorescence intensity and concentration of PPL-B. Indicating that fluorescence quenching of PPL-B is not caused by aggregation.

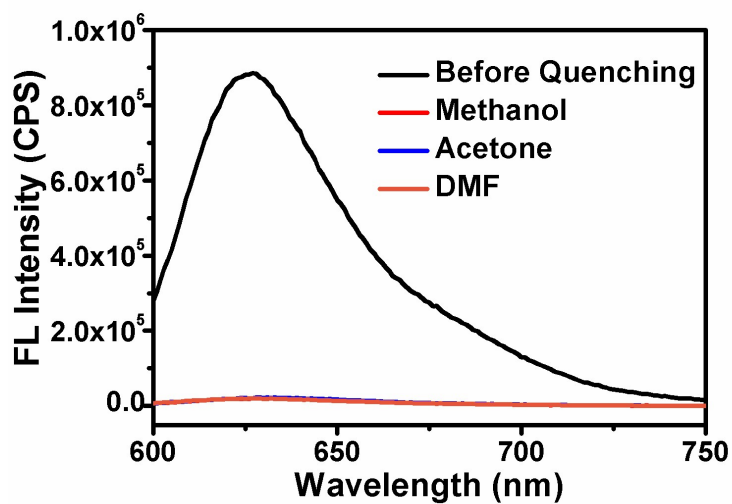


Fig. S14 Fluorescence of CUR@PPL-B co-assembled with different solvent. Indicating that solvent used in co-assemble experiment cannot induce fluorescence quenching of PPL-B.

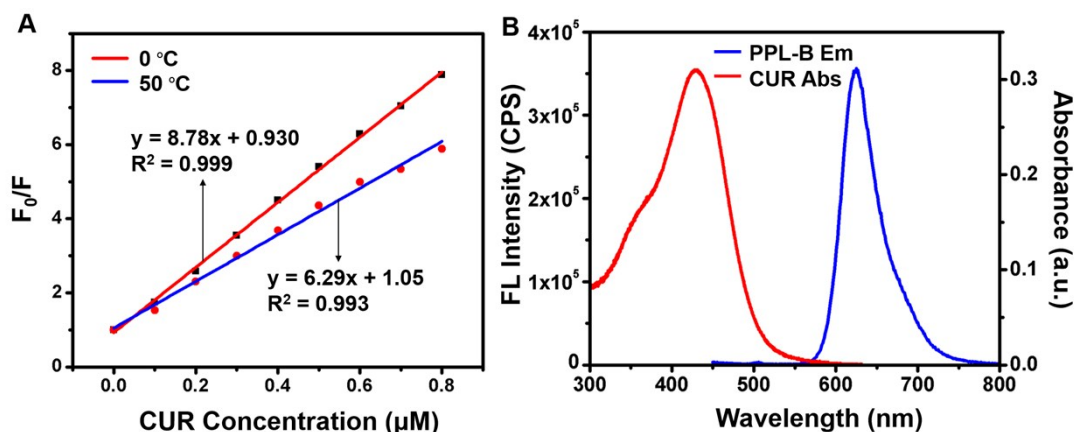


Fig. S15 (A) Stern-Volmer plots for fluorescence quenching of PPL-B at 0 °C and 50 °C. (B) Fluorescence spectrum of PPL-B and UV-vis absorption of CUR.

Stern-Volmer measurement

Fluorescence quenching includes dynamic quenching and static quenching according to different quenching mechanisms. Dynamic quenching is due to the collision between fluorophore and quencher molecule, while static quenching is accompanied by the formation of ground-state complex.¹ Generally, a linear Stern-Volmer plot indicates that one of the two mechanisms is predominant. In contrast, a curved Stern-Volmer plot implies the combination of dynamic quenching and static quenching.² Therefore, Stern-Volmer model was used to study the fluorescence quenching mechanism of PPL-B. The Stern-Volmer plot displays linearity (Fig. S15A, ESI†), and the K_{SV} value is 8.78×10^6 L/mol under 0 °C. Such a large K_{SV} value and the linear Stern-Volmer plot imply that static quenching is the main reason for fluorescence quenching of PPL-B. To confirm the assumption, K_{SV} value under 50 °C was also measured and a smaller K_{SV} value was obtained. The phenomenon that K_{SV} decreased as the temperature went up further verified the static quenching mechanism.^{1,3,4}

Generally, the static quenching is caused by the following possible mechanisms: fluorescence resonance energy transfer (FRET), photo-induced electron transfer (PET) and redox-induced electron transfer.¹ Firstly, because the absorbance spectrum of CUR and the fluorescence spectrum of PPL-B don't overlap (Fig. S15B, ESI†), FRET mechanism can be excluded for the fluorescence quenching of PPL-B.⁵ In addition, both PPL-B and CUR possess neither strong reductibility nor strong oxidability in neutral aqueous solution. Thus, the redox reaction could hardly take place between PPL-B and CUR. As a consequence, PET mechanism is the only probable one that accounts for the fluorescence quenching of PPL-B, which confirms our hypothesis.

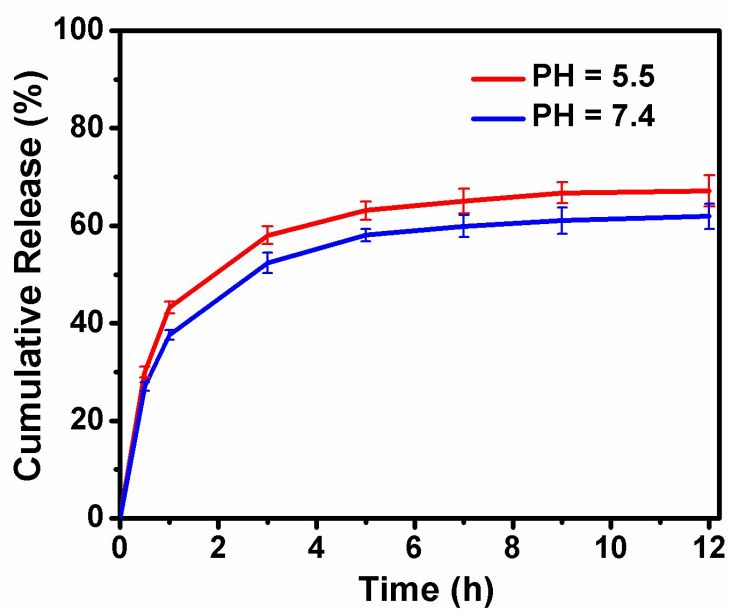


Fig. S16 *In vitro* drug release profiles of CUR@PPL-B in PBS of different pH values. Under the experiment condition, pH value has little influence on drug release profile.

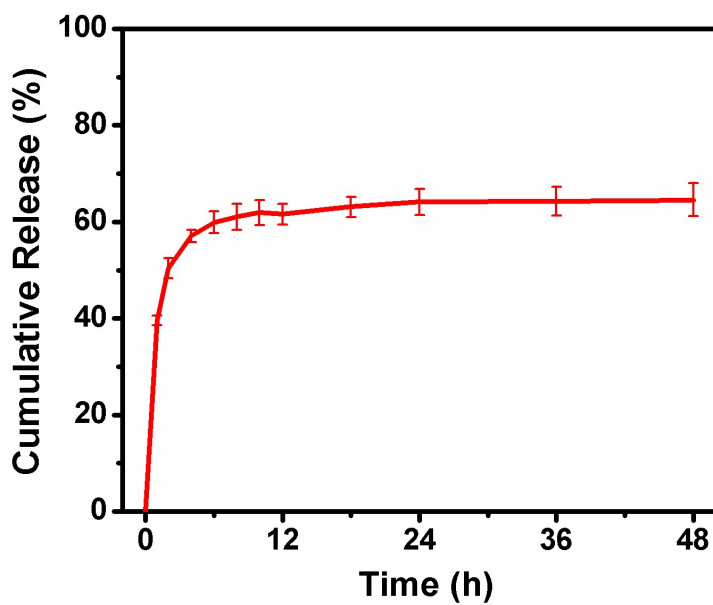


Fig. S17 *In vitro* long-term drug release profile of CUR@PPL-B.

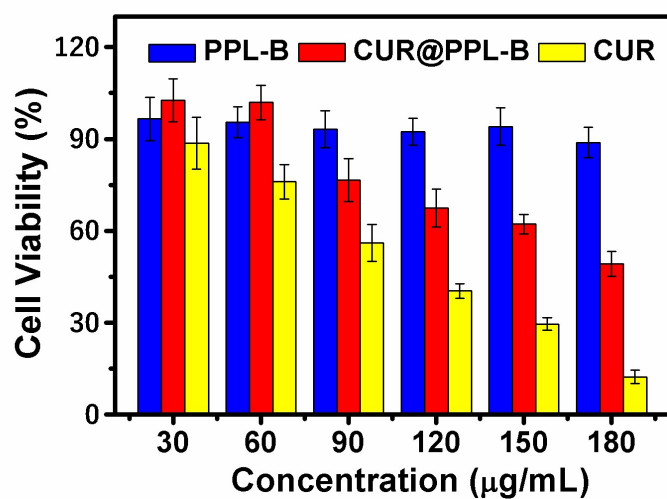


Fig. S18 Cell viability assay of PPL-B, CUR@PPL-B and CUR with HeLa cells. CUR@PPL-B and CUR both show obvious cytotoxicity against HeLa cells.

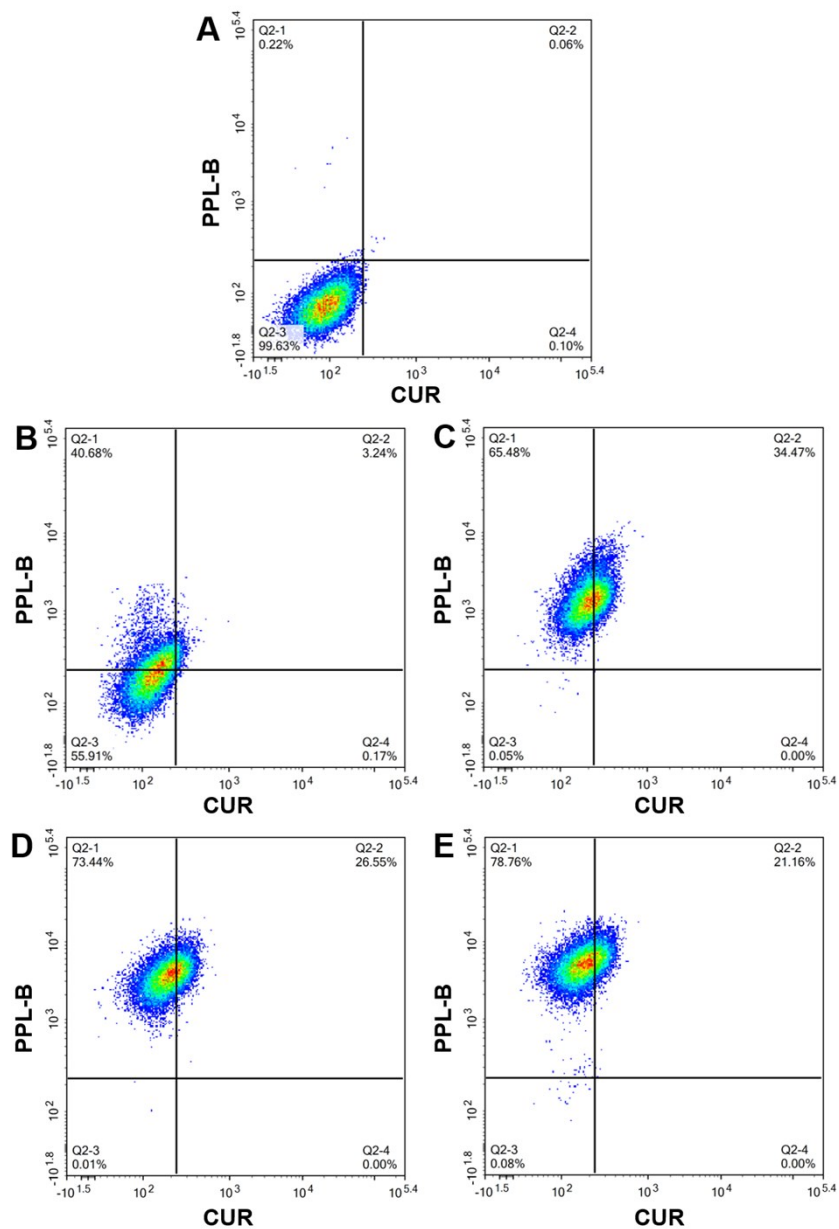


Fig. S19 Flow cytometry analysis of CUR@PPL-B. (A) Blank. (B) 1 h. (C) 6 h. (D) 12 h. (E) 18 h. CUR channel: excited at 405 nm and detected at 530 nm. PPL-B channel: excited at 633 nm and detected at 660 nm.

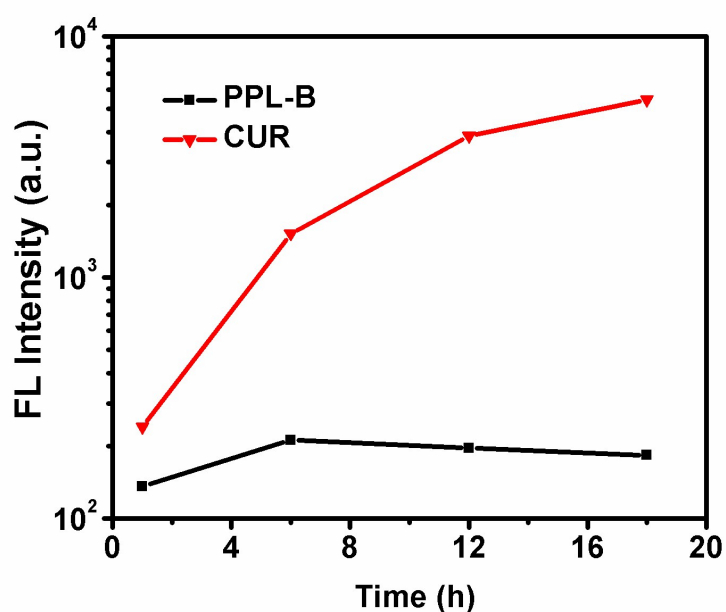


Fig. S20 Fluorescence change of HeLa cells incubated with CUR@PPL-B (Red line: PPL-B channel; Black line: CUR channel). Fluorescence intensity of PPL-B enhances obviously with time, while CUR's fluorescence only shows limited enhancement, which may be due to the quick degradation of CUR under laser irradiation.

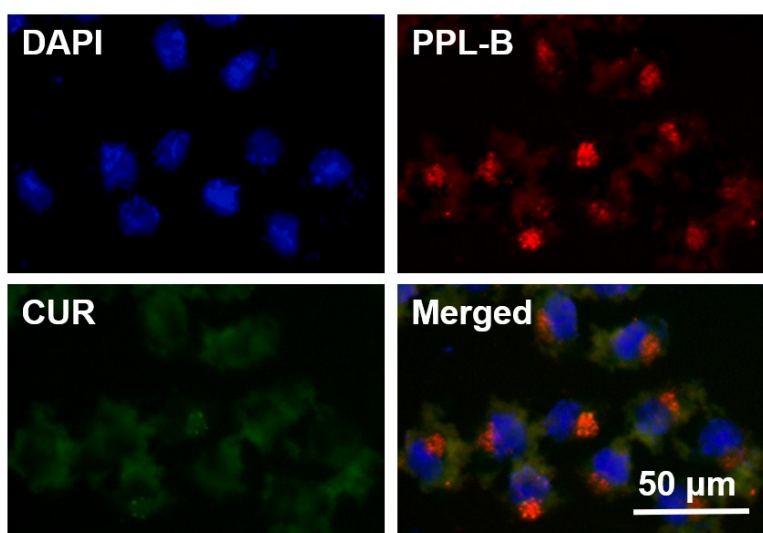


Fig. S21 Intracellular localization of CUR@PPL-B and DAPI. In this experiment, HeLa cells were firstly incubated with CUR@PPL-B (50 $\mu\text{g}/\text{mL}$) for 1 h, after which the culture medium in each well was replaced with fresh one. Then, DAPI was added to the wells after 12 h incubation. 0.5 h later, these wells were washed with PBS and the fluorescent images were captured.

Reference:

- 1 Y. Zhang, Y. Zhang, W. Yang, L. Bian, *Talanta*, 2018, **188**, 7-16.
- 2 S. Chaudhary, H. Sharma, M. D. Milton, *Chemistryselect*, 2018, **3**, 4598-4608.
- 3 J. Pan, Y. Wang, C. Zhang, X. Wang, H. Wang, J. Wang, Y. Yuan, X. Wang, X. Zhang, C. Yu, S. K. Sun, X. P. Yan, *Adv. Mater.*, 2018, **30**, 1704408.
- 4 L. Miyan, Zulkarnain, A. Ahmad, *J. Mol. Liq.*, 2018, **262**, 514-526.
- 5 J. Wang, P. P. Gao, X. X. Yang, T. T. Wang, J. Wang, C. Z. Huang, *J. Mater. Chem. B*, 2014, **2**, 4379-4386.